Hindawi
Mathematical Problems in Engineering
Volume 2019, Article ID 4596782, 14 pages
https://doi.org/10.1155/2019/4596782

Research Article

Takagi-Sugeno Fuzzy Modeling and PSO-Based Robust LQR Anti-Swing Control for Overhead Crane

Xuejuan Shao,[1,2] **Jinggang Zhang**,[1] **and Xueliang Zhang**[3]

[1]*College of Electronic Information Engineering, Taiyuan University of Science and Technology, Taiyuan 030024, China*
[2]*Shanxi Key Laboratory of Advanced of Advanced Control and Intelligent Information System, Taiyuan 030024, China*
[3]*College of Mechanical Engineering, Taiyuan University of Science and Technology, Taiyuan 030024, China*

Correspondence should be addressed to Jinggang Zhang; jg_zhang65@163.com

Received 4 January 2019; Revised 5 March 2019; Accepted 17 March 2019; Published 4 April 2019

Academic Editor: Jorge Rivera

The dynamic model of overhead crane is highly nonlinear and uncertain. In this paper, Takagi-Sugeno (T-S) fuzzy modeling and PSO-based robust linear quadratic regulator (LQR) are proposed for anti-swing and positioning control of the system. First, on the basis of sector nonlinear theory, the two T-S fuzzy models are established by using the virtual control variables and approximate method. Then, considering the uncertainty of the model, robust LQR controllers with parallel distributed compensation (PDC) structure are designed. The feedback gain matrices are obtained by transforming the stability and robustness of the system into linear matrix inequalities (LMIs) problem. In addition, particle swarm optimization (PSO) algorithm is used to overcome the blindness of LQR weight matrix selection in the design process. The proposed control methods are simple, feasible, and robust. Finally, the numeral simulations are carried out to prove the effectiveness of the methods.

1. Introduction

Overhead crane is a popular underactuated mechanical system, which is widely used to carry and lift goods indoors or outdoors. The working process is divided into three stages: load rising, horizontal transportation, and load decreasing. Its control goal is to transport the goods quickly to the desired position without residual swing at the end. In the process of transporting goods, if the length of rope and the load mass remain unchanged and the external interference does not exist, the load swing is mainly caused by the motion of the trolley. However, the rope length and load mass often change accordingly due to the need of transportation task. The disturbance of external environment, such as friction and wind force, may also affect the anti-swing and positioning performance of the control system for the crane used outdoors. So it is necessary to design a controller that can reduce or suppress the uncertainty of the system.

At present, there are many methods for anti-swinging and positioning control of cranes. Generally speaking, according to the crane model, the control methods for crane systems are divided into two main categories. One is linear control methods based on linearization model, including input shaping [1–3], trajectory planning [4–6], PID control [7–9], internal model control [10], etc. In order to reduce the complexity of controller design or stability analysis, these control methods first linearize the complex nonlinear model near the equilibrium point or ignore some specific nonlinear coupling terms. The other is the control method based on nonlinear model, such as nonlinear coupled control method [11], sliding model control [12, 13], robust control [14], model predictive control [15–17], nonlinear control method for complicated operation duties [18], and so on. Most of these control methods do not consider the uncertainty of the system, and the robustness is relatively poor. Sliding mode control [19, 20] can effectively deal with the influence of system uncertainty, but the convergence analysis of sliding mode surface is needed.

In recent years, the T-S modeling and control method based on the T-S fuzzy model have been highly concerned by the control community. T-S fuzzy model is a combination of some linear models. Therefore, the theory and method of

linear systems can be used to deal with the nonlinear problem. In addition, the linear function or the constant function can be calculated, and the calculation efficiency is relatively high. At present, the T-S modeling and control method have been successfully applied to many nonlinear systems, such as inverted pendulum system [21–23], the ball bar system [24, 25], solar photovoltaic power system [26], aircraft motion control system [27] and helicopter system [28], vehicle system [29–31], micro hydropower plant prototype system [32], nonlinear systems with persistent bounded disturbances [33], and so on. However, the modeling and control method is relatively rare in cranes. In [34, 35], the T-S fuzzy model of the crane is obtained by the local approximation method. On the basis of the model, H-infinity anti-swing controller and guaranteed cost controller are designed, respectively. The controller designed according to the local approximate model cannot guarantee the global stability of the system. In [36], a guaranteed cost fuzzy controller with input/state constraints is designed for overhead cranes, in which the traditional T-S fuzzy systems are replaced by fuzzy description systems. This method can eliminate the residual swing angle of the load, but the uncertainty of the system model is not considered when designing the controller.

In order to solve the nonlinear and uncertain problems of dynamics model, a novel anti-swing and positioning control method for overhead crane is presented in this paper. On the basis of sector nonlinear theory, the two kinds of T-S fuzzy models are established by using the virtual control variables and approximate method. The nonlinear models of cranes can be regarded as a combination of a series of linear models. The rope length, load mass, and friction between the trolley and the track may change in the process of transporting goods. In order to make the system have strong robustness, robust LQR controllers considering uncertainty are designed. The weight matrix of LQR will affect the control performance of the system, so PSO algorithm is proposed to solve the problem. The LQR controller in [37] and the robust LQR controller [34] are used to compare the control effect. The results show that the proposed robust LQR controllers have better robustness and rejected disturbance ability.

The contributions of this study are as follows:

(1) The processing method of nonlinear model is proposed. A method using virtual control variables and a new approximation method are used in the establishment of T-S model.

(2) Aiming at the anti-swing and positioning control of overhead crane, a robust LQR control method is presented on the basis of T-S fuzzy models considering uncertainty.

(3) A weighted matrix selection method based on PSO algorithm is proposed.

(4) The system has good anti-swing and positioning control performance and strong robustness to uncertain factors.

The remaining of this paper is organized as follows. In Section 2, two T-S fuzzy models for overhead cranes are presented. Section 3 addresses the design of the PSO-based robust LQR fuzzy controller. Numerical simulation results are shown in Section 4. Section 5 concludes the paper.

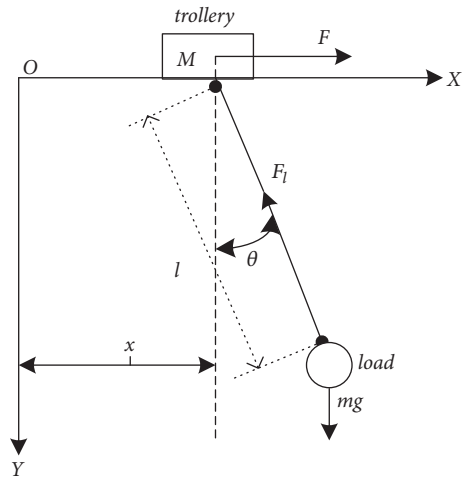

Figure 1: Description of overhead crane system.

2. The Mathematical Model of Overhead Crane

The overhead crane system is mainly used to lift and move goods. The purpose of its control is to quickly and accurately transport the goods to the desired position without residual swing at the target position. When there is external disturbance, the swing angle can be limited to a certain range. The overhead system is mainly made up of three parts: a trolley, a rope, and a payload. The structure of a two-dimensional overhead crane system is shown in Figure 1, where F and F_l represent the actuating force acted on the trolley and the force in vertical direction, respectively; x is the horizontal position of the trolley; M and m are the mass of the trolley and the payload, respectively; l is the length of the rope; θ is the swing angle of the payload; and g denotes the gravitation acceleration.

In this study, it is assumed that the mass and elasticity of the rope are ignored, the length of the rope remains constant during the moving process of the trolley, and the payload and trolley are regarded as the point mass. Then, the nonlinear dynamic model of two-dimensional overhead crane with constant rope length can be obtained as follows [6]:

$$(M+m)\,\ddot{x} + ml\ddot{\theta}\cos\theta - ml\dot{\theta}^2\sin\theta + \mu\dot{x} = F \tag{1}$$

$$ml^2\ddot{\theta} + ml\ddot{x}\cos\theta + mgl\sin\theta = 0 \tag{2}$$

where μ is the damping coefficient on the trolley.

Choosing the state variables as $\mathbf{x} = \begin{bmatrix} x_1 & x_2 & x_3 & x_4 \end{bmatrix}^T = \begin{bmatrix} x & \dot{x} & \theta & \dot{\theta} \end{bmatrix}^T$, the state equations of the overhead crane are written as

$$\begin{aligned}
\dot{x}_1 &= x_2 \\
\dot{x}_2 &= \frac{mg\sin x_3\cos x_3 + mlx_4{}^2\sin x_3 - \mu x_2 + F}{(M+m) - m\cos^2 x_3} \\
\dot{x}_3 &= x_4 \\
\dot{x}_4 &= \frac{(M+m)\,g\sin x_3 + mlx_4{}^2\sin x_3\cos x_3 - \mu x_2\cos x_3 + F\cos x_3}{[m\cos^2 x_3 - (M+m)]\,l}
\end{aligned} \tag{3}$$

It is obvious that the overhead crane is a nonlinear system and there are five nonlinear terms in (3). According to T-S fuzzy model theory, $2^5 = 32$ fuzzy rules are required. In order to simplify the nonlinear mathematical model and reduce the number of premise variables, the following two methods are used to deal with the above-mentioned state equation (3).

2.1. Virtual Control Variable Method. Now let F in (3) be the following form:

$$F = \left(M + m\sin^2 x_3\right)u - mg\sin x_3\cos x_3 - mlx_4{}^2\sin x_3 \tag{4}$$

where u is a virtual control variable.

Substituting (4) into (3), (3) is simplified to

$$\begin{aligned}
\dot{x}_1 &= x_2\\
\dot{x}_2 &= \frac{-\mu x_2 l}{\left[m\cos^2 x_3 - (M+m)\right]l} + u\\
\dot{x}_3 &= x_4\\
\dot{x}_4 &= -\frac{g\sin x_3}{l} - \frac{\mu x_2\cos x_3}{\left[ml\cos^2 x_3 - (M+m)\right]l} - \frac{\cos x_3}{l}u
\end{aligned} \tag{5}$$

As can be seen from (5), there are three nonlinear terms which are defined as premise variables z_{11}, z_{12}, and z_{13} respectively; that is,

$$\begin{aligned}
z_{11} &= \sin x_3,\\
z_{12} &= \cos x_3,\\
z_{13} &= \frac{1}{ml\cos^2 x_3 - (M+m)l}.
\end{aligned} \tag{6}$$

According to the theorem of sector nonlinearity, the membership functions associated with the premise variables can be determined by the following equations (7)-(12).

$$z_{11}(t) = \sum_{k=1}^{2} M_{1k}\left(z_{11}(t)\right)a_k x_3(t) \tag{7}$$

$$z_{12}(t) = \sum_{j=1}^{2} N_{1j}\left(z_{12}(t)\right)b_j \tag{8}$$

$$z_{13}(t) = \sum_{n=1}^{2} R_{1n}\left(z_{13}(t)\right)c_n \tag{9}$$

and

$$M_{11}\left(z_{11}(t)\right) + M_{12}\left(z_{11}(t)\right) = 1 \tag{10}$$

$$N_{11}\left(z_{12}(t)\right) + N_{12}\left(z_{12}(t)\right) = 1 \tag{11}$$

$$R_{11}\left(z_{13}(t)\right) + R_{12}\left(z_{13}(t)\right) = 1 \tag{12}$$

To ensure the safety of the transportation process, some restrictive conditions such as $|\theta(t)| \le \theta_p$ (rad) and $|\dot{\theta}(t)| \le \theta_v$ (rad/s) are given, where θ_p and θ_v are the maximum swing angle and the maximum swing angular velocity of the load, respectively. So

$$\begin{aligned}
a_1 &= a_{\max} = 1,\\
a_2 &= a_{\min} = \frac{1}{\theta_p}\sin\theta_p,\\
b_1 &= b_{\max} = 1,\\
b_2 &= b_{\min} = \cos\theta_p,\\
c_1 &= c_{\max} = \frac{1}{ml\cos^2\theta_p - (M+m)l},\\
c_2 &= c_{\min} = \frac{1}{ml - (M+m)l}.
\end{aligned} \tag{13}$$

By (7)-(12), the membership functions can be calculated as

$$M_{11}\left(z_{11}(t)\right) = \begin{cases} \dfrac{z_{11}(t) - \left(1/\theta_p\right)\sin\theta_p\sin^{-1}\left(z_{11}(t)\right)}{1 - \left(1/\theta_p\right)\sin\theta_p\sin^{-1}\left(z_{11}(t)\right)} & \text{if } z_{11}(t) \ne 0\\ 1 & \text{otherwise} \end{cases} \tag{14}$$

$$M_{12}\left(z_{11}(t)\right) = 1 - M_{11}\left(z_{11}(t)\right) \tag{15}$$

$$N_{11}\left(z_{12}(t)\right) = \frac{z_{11}(t) - b_2}{b_1 - b_2} \tag{16}$$

$$N_{12}\left(z_{12}(t)\right) = 1 - N_{11}\left(z_{12}(t)\right) \tag{17}$$

$$R_{11}\left(z_{13}(t)\right) = \frac{z_{13}(t) - c_2}{c_1 - c_2} \tag{18}$$

$$R_{12}\left(z_{13}(t)\right) = 1 - R_{11}\left(z_{13}(t)\right) \tag{19}$$

2.2. Approximated Method. Equation (3) can also be written as follows:

$$\begin{bmatrix}\dot{x}_1\\ \dot{x}_2\\ \dot{x}_3\\ \dot{x}_4\end{bmatrix} = \begin{pmatrix} 0 & 1 & 0 & 0\\ 0 & \dfrac{-\mu}{M + m\sin^2 x_3} & \dfrac{mg\cos x_3\sin x_3}{\left(M + m\sin^2 x_3\right)x_3} & \dfrac{mlx_4\sin x_3}{M + m\sin^2 x_3}\\ 0 & 0 & 0 & 1\\ 0 & \dfrac{\mu\cos x_3}{l\left(M + m\sin^2 x_3\right)} & \dfrac{-(M+m)g\sin x_3}{l\left(M + m\sin^2 x_3\right)x_3} & \dfrac{-mx_4\sin x_3\cos x_3}{M + m\sin^2 x_3} \end{pmatrix}\begin{bmatrix}x_1\\ x_2\\ x_3\\ x_4\end{bmatrix} + \begin{pmatrix} 0\\ \dfrac{1}{M + m\sin^2 x_3}\\ 0\\ \dfrac{-\cos x_3}{l\left(M + m\sin^2 x_3\right)} \end{pmatrix}F \tag{20}$$

Assuming that the load swing angle is small and satisfies the following approximate relationship $\lim_{x_3 \to 0}(\sin x_3 / x_3) = 1$, then (20) can be simplified as

$$\begin{bmatrix} \dot{x}_1 \\ \dot{x}_2 \\ \dot{x}_3 \\ \dot{x}_4 \end{bmatrix} = \begin{pmatrix} 0 & 1 & 0 & 0 \\ 0 & \dfrac{-\mu}{M + m\sin^2 x_3} & \dfrac{mg\cos x_3}{M + m\sin^2 x_3} & \dfrac{mlx_4 \sin x_3}{M + m\sin^2 x_3} \\ 0 & 0 & 0 & 1 \\ 0 & \dfrac{\mu \cos x_3}{l(M + m\sin^2 x_3)} & \dfrac{-(M+m)g}{l(M + m\sin^2 x_3)} & \dfrac{-mx_4 \sin x_3 \cos x_3}{M + m\sin^2 x_3} \end{pmatrix} \begin{bmatrix} x_1 \\ x_2 \\ x_3 \\ x_4 \end{bmatrix} + \begin{pmatrix} 0 \\ \dfrac{1}{M + m\sin^2 x_3} \\ 0 \\ \dfrac{-\cos x_3}{l(M + m\sin^2 x_3)} \end{pmatrix} F \tag{21}$$

Define the premise variables as follows:

$$\begin{aligned} z_{21} &= \frac{1}{M + m\sin^2 x_3} = \sum_{k=1}^{2} M_{2k}(z_{21}(t))\, p_k \\ z_{22} &= \cos x_3 = \sum_{j=1}^{2} N_{2j}(z_{22}(t))\, b_j \\ z_{23} &= x_4 \sin x_3 = \sum_{n=1}^{2} R_{2n}(z_{23}(t))\, d_n \end{aligned} \tag{22}$$

where

$$\begin{aligned} p_1 &= \max z_{21} = \frac{1}{M}, \\ p_2 &= \min z_{21} = \frac{1}{M + m\sin^2 \theta_p}, \\ b_1 &= \max z_{22} = 1, \\ b_2 &= \min z_{22} = \cos \theta_p, \\ d_1 &= \max z_{23} = \theta_v \sin \theta_p, \\ d_2 &= \min z_{23} = -\theta_v \sin \theta_p. \end{aligned} \tag{23}$$

The membership function of each premise variable has the following relationship.

$$\begin{aligned} M_{21}(z_{21}(t)) + M_{22}(z_{21}(t)) &= 1 \\ N_{21}(z_{22}(t)) + N_{22}(z_{22}(t)) &= 1 \\ R_{21}(z_{23}(t)) + R_{22}(z_{23}(t)) &= 1 \end{aligned} \tag{24}$$

The membership function can be obtained from (22) and (24).

$$\begin{aligned} M_{21} &= \frac{p_1 - z_{21}}{p_1 - p_2}, \\ M_{22} &= 1 - M_{21}; \\ N_{21} &= \frac{b_1 - z_{22}}{b_1 - b_2}, \\ N_{22} &= 1 - N_{21}; \\ R_{21} &= \frac{d_1 - z_{23}}{d_1 - d_2}, \\ R_{22} &= 1 - R_{21}. \end{aligned} \tag{25}$$

2.3. T-S Fuzzy Model. From the above analysis, we can see that the rule-base for T-S fuzzy model obtained by the above two methods is composed of $2^3 = 8$ rules. The fuzzy rules are as follows:

Rule i.

$$\begin{aligned} &IF \quad z_{l1}(t) \ \ is \ M_{lk}, \\ &\qquad z_{l2}(t) \ \ is \ N_{lj} \\ &\qquad AND \ z_{l3}(t) \ \ is \ R_{ln} \\ &THEN \quad \dot{\mathbf{x}}(t) = \mathbf{A}_{li}\mathbf{x}(t) + \mathbf{B}_{li}\mathbf{u}(t) \\ &\quad l = 1,2; \ i = 1,2,\ldots 8; \ k = 1,2; \ j = 1,2; \ n = 1,2 \end{aligned} \tag{26}$$

The T-S fuzzy models can be expressed as

$$\dot{\mathbf{x}}(t) = \sum_{i=1}^{r} h_{li}(\mathbf{z}(t)) \left[\mathbf{A}_{li}\mathbf{x}(t) + \mathbf{B}_{li}\mathbf{u}(t)\right] \qquad l = 1,2; \ i = 1,2,\ldots,r = 8 \tag{27}$$

$$y(t) = \sum_{i=1}^{r} h_{li}(\mathbf{z}(t))\, C_{li}\mathbf{x}(t)$$

where

$$\begin{aligned} \sum_{\mathbf{i}=1}^{\mathbf{r}} h_{li}(\mathbf{z}(\mathbf{t})) &= \frac{\sum_{\mathbf{i}=1}^{\mathbf{r}} \omega_{li}(\mathbf{z}(\mathbf{t}))}{\sum_{\mathbf{i}=1}^{\mathbf{r}} \omega_{li}(\mathbf{z}(\mathbf{t}))} \\ \omega_{li}(\mathbf{z}(\mathbf{t})) &= \prod_{\mathbf{j}=1}^{3} M_{li}(\mathbf{z}(\mathbf{t})) \end{aligned} \tag{28}$$

ω_{li} represents the weight of the ith rule, $i = 1,2,\ldots,r, r = 8$, $\mathbf{z}(t) = \{z_{l1}(t) \ \ z_{l2}(t) \ \ z_{l3}(t)\}$ is the system input which belongs

to the premise variable, and $h_{li}(t)$ can be regarded as the normalized weight of each rule and it satisfies

$$\sum_{i=1}^{r} h_{li}(\mathbf{z}(t)) = 1 \tag{29}$$

3. The Design of PSO-Based Robust LQR Controller

On the basis of the previous T-S fuzzy models, the corresponding T-S fuzzy model with uncertainty is given as follows:

$$\begin{aligned}\dot{x}(t) &= \sum_{i=1}^{r} \left(A_{li} + D\Delta(t) E_{ai}\right) x(t) \\ &\quad + \left(B_{li} + D\Delta(t) E_{bi}\right) u(t) \\ y(t) &= \sum_{i=1}^{r} h_{li}(x(t)) C_{li} x(t) \\ &\quad l = 1,2;\ i = 1,2,\ldots,r,\ r = 8.\end{aligned} \tag{30}$$

D, E_{ai} and E_{bi} are constant matrices reflecting the uncertainty of parameters in the system model, and uncertain matrix $\Delta(t) \in R^{i\times j}$ satisfies

$$\Delta(t)^T \Delta(t) \le I \tag{31}$$

For system (30), a performance index is defined as

$$J = \int_0^\infty \left[y^T(t) Q y(t) + u^T(t) R u(t)\right] dt, \tag{32}$$

where Q and R are positive definite weighting matrices.

The control law of each subsystem is similar to rules defined in the T-S fuzzy model and has the same membership function and the premise part of rules.

Rule i.

$$\begin{aligned}&IF \quad z_{l1}(t) \ is\ M_{lk}, \\ &\quad z_{l2}(t) \ is\ N_{lj} \\ &\quad and\ z_{l3}(t) \ is\ R_{ln}, \\ &\quad\quad l = 1,2;\ k = 1,2;\ j = 1,2;\ n = 1,2; \\ &THEN \quad u(t) = -K_{li}\overline{\mathbf{x}}(t), \quad i = 1,2,\cdots,8.\end{aligned} \tag{33}$$

$\overline{\mathbf{x}}(t) = \left[x(t) - x_d \ \ \dot{x}(t) \ \ \theta(t) \ \ \dot{\theta}(t)\right]$, $K_i (i = 1,\cdots,8)$.

The control law of the whole system is defined as

$$u(t) = -\sum_{i=1}^{8} h_{li}(\mathbf{z}(t)) K_{li}\overline{\mathbf{x}}(t) \tag{34}$$

When the T-S fuzzy model obtained by the first method is used, (34) need be substituted into (4), and the resulting F is added to the overhead crane as a control input. When using the above second T-S model, F equals u. So u can be used as the control input directly.

3.1. Design of Robust LQR Controller. Sufficient conditions for the existence of fuzzy control law in uncertain continuous system (30) are given in the following lemma.

Lemma 1. *For the system described in (30), if there is a positive definite matrix P and a positive semidefinite matrix Q_0, it satisfies*

$$U_{ii} + (s-1) Q_3 < 0, \tag{35}$$

$$\begin{aligned}V_{ij} - 2Q_4 < 0, \quad i < j, \\ s.t.\ h_i \cap h_j \ne \phi, \quad s > 1,\end{aligned} \tag{36}$$

then the PDC structure controller can be used to make it stable and the performance index (32) can be satisfied

$$J < x^T(0) P x(0) \tag{37}$$

where

$$U_{ii} = \begin{bmatrix} S_\Delta & C_i^T & -F_i^T \\ * & -W^{-1} & 0 \\ * & * & -R^{-1} \end{bmatrix}$$

$$V_{ij} = \begin{bmatrix} Z_\Delta & C_i^T & -F_j^T & C_j^T & -F_i^T \\ * & -W^{-1} & 0 & 0 & 0 \\ * & * & -R^{-1} & 0 & 0 \\ * & * & * & -W^{-1} & 0 \\ * & * & * & * & -R^{-1} \end{bmatrix}$$

$$\begin{aligned}S_\Delta &= \left[A_i + D\Delta(t) E_{ai} - \left(B_i + D\Delta(t) E_{bi}\right) F_i\right]^T P \\ &\quad + P\left[A_i + D\Delta(t) E_{ai} - \left(B_i + D\Delta(t) E_{bi}\right) F_i\right] \\ Z_\Delta &= \left[A_i + D\Delta(t) E_{ai} - \left(B_i + D\Delta(t) E_{bi}\right) F_j\right]^T P \\ &\quad + P\left[A_i + D\Delta(t) E_{ai} - \left(B_i + D\Delta(t) E_{bi}\right) F_j\right] \\ &\quad + \left[A_j + D\Delta(t) E_{aj} - \left(B_j + D\Delta(t) E_{bj}\right) F_i\right]^T P \\ &\quad + P\left[A_j + D\Delta(t) E_{aj} - \left(B_j + D\Delta(t) E_{bj}\right) F_i\right] \\ Q_3 &= \mathrm{diag}\{Q_0, 0, 0\}, \\ Q_4 &= \mathrm{diag}\{Q_0, 0, 0, 0\}\end{aligned} \tag{38}$$

U_{ij} and V_{ij} are block symmetric matrices.

Lemma 2. *If there are appropriate dimension matrices Y, D, and E, where Y is symmetric, then for all matrices $\Delta(t)$ satisfying $\Delta^T(t)\Delta(t) \le I$, if and only if there is a constant ε such that the following inequality holds*

$$Y + DD^T + \varepsilon^{-1} E^T E < 0 \tag{39}$$

The following theorem transforms the robust LQR control law problem given by Lemma 1 into a solvability problem for linear matrix inequality.

Theorem 3. *For the system described by (30), if matrices X, M_i, and Y_0 and scalars $\varepsilon_i > 0$ and $\varepsilon_{ij} > 0$ $(i < j)$, where X is a symmetric positive matrix and Y_0 is a symmetric positive semidefinite matrix, satisfy the following inequalities*

$$U_{ii} + (s-1)\, Y_4 < 0, \tag{40}$$

$$\begin{aligned} V_{ij} - 2Y_5 < 0, \quad i < j, \\ s.t.\ h_i \cap h_j \neq \phi, \end{aligned} \tag{41}$$

then the controller with PDC structure can be used to stabilize system (30) and to make the performance index (32) satisfy the following inequality:

$$J < x^T(0)\, X^{-1} x(0) \tag{42}$$

where

$$s > 1;$$

$$i, j = 1, 2, \ldots, r;$$

$$U_{ii} = \begin{bmatrix} S_\Delta & XC_i^T & -M_i^T & XE_{ai}^T - M_i^T E_{bi}^T \\ * & -W^{-1} & 0 & 0 \\ * & * & -R^{-1} & 0 \\ * & * & * & -\varepsilon_i I \end{bmatrix},$$

$$V_{ij} = \begin{bmatrix} Z_\Delta & XC_i^T & -M_j^T & XC_j^T & -M_i^T & T_\Delta \\ * & -W^{-1} & 0 & 0 & 0 & 0 \\ * & * & -R^{-1} & 0 & 0 & 0 \\ * & * & * & -W^{-1} & 0 & 0 \\ * & * & * & * & -R^{-1} & 0 \\ * & * & * & * & * & -\varepsilon_{ij} I \end{bmatrix}, \tag{43}$$

$$S_\Delta = XA_i^T + A_i X + \varepsilon_i DD^T - B_i M_i - M_i^T B_i^T,$$

$$\begin{aligned} Z_\Delta = {} & XA_i^T + A_i X + \varepsilon_{ij} DD^T - B_i M_j - M_j^T B_i{}^T \\ & + XA_j^T + A_j X - B_j M_i - M_i^T B_j^T, \end{aligned}$$

$$T_\Delta = XE_{ai}^T + XE_{aj}^T - M_i{}^T E_{bj}^T - M_j^T E_{bj}^T,$$

$$Y_5 = \operatorname{diag}\{Y_0, 0, 0, 0, 0, 0\},$$

$$Y_4 = \operatorname{diag}\{Y_0, 0, 0, 0\}.$$

Proof. Multiplying both sides of (40) by matrix $\operatorname{diag}\{P^{-1}, I, I\}$ and defining some new variables $X = P^{-1}$, $Y_0 = XQ_0X$, and $M_i = F_iX$, we can obtain

$$\begin{bmatrix} H_\Delta & XC_i^T & -F_i^T \\ * & -W^{-1} & 0 \\ * & * & -R^{-1} \end{bmatrix} + (s-1)\operatorname{diag}\{Y_0, 0, 0\} < 0, \tag{44}$$

where

$$\begin{aligned} H_\Delta = {} & X\left[A_i + D\Delta(t)\, E_{ai}\right]^T + \left[A_i + D\Delta(t)\, E_{ai}\right] X \\ & - \left[B_i + D\Delta(t)\, E_{bi}\right] M_i \\ & - M_i^T \left[B_i + D\Delta(t)\, E_{bi}\right]^T \end{aligned} \tag{45}$$

So the above inequality can be further written as

$$\begin{aligned} U_{ii} + (s-1)\, Y_3 + {} & \begin{bmatrix} D \\ 0 \\ 0 \end{bmatrix} \Delta(t) \begin{bmatrix} XE_{ai}^T - M_i^T E_{bi}^T \\ 0 \\ 0 \end{bmatrix}^T \\ & + \begin{bmatrix} XE_{ai}^T - M_i^T E_{bi}^T \\ 0 \\ 0 \end{bmatrix} \Delta^T(t) \begin{bmatrix} D \\ 0 \\ 0 \end{bmatrix}^T < 0, \end{aligned} \tag{46}$$

where

$$U_{ii} = \begin{bmatrix} XA_i^T + A_i X - B_i M_i - M_i^T B_i^T & XC_i^T - M_i^T & \\ * & -W^{-1} & 0 \\ * & * & -R^{-1} \end{bmatrix}, \tag{47}$$

$$Y_3 = \operatorname{diag}\{Y_0, 0, 0, 0\}$$

According to Lemma 2 and the Schur complement property of matrices, the above inequality holds all allowable uncertainties. If and only if there exists $\varepsilon_i > 0$, then (40) holds.

Similarly, inequality (41) can be proved. Therefore, Theorem 3 can be obtained from Lemma 1.

In short, in order to minimize the upper bound of performance index J, the control law can be obtained by solving the following LMIs problem.

$$\begin{aligned} \min_{X, M_i, \varepsilon_i, \varepsilon_{ij}} \quad & \lambda \\ s.t. \quad & \text{(a) } X > 0,\ Y_0 \geq 0,\ \varepsilon_i > 0,\ \varepsilon_{ij} > 0, \\ & \text{(b) Inequalities (35) and (36)} \\ & \text{(c) } \begin{bmatrix} \lambda & x^T(0) \\ x(0) & X \end{bmatrix} > 0 \end{aligned} \tag{48}$$

□

3.2. PSO-Based Robust LQR Controller Optimization. The weigh matrices Q and R determine the feedback gains which have great influence on the performance of control system. According to the model of the overhead crane, it can be seen that the system has four state variables and one input variable, so Q is a 4×4 positive semidefinite symmetric matrix, and R is a constant positive definite matrix. In this paper, Q and R are as follows:

$$\begin{aligned} Q &= \operatorname{diag}\left[q_{11}, q_{22}, q_{33}, q_{44}\right] \\ R &= [r] \end{aligned} \tag{49}$$

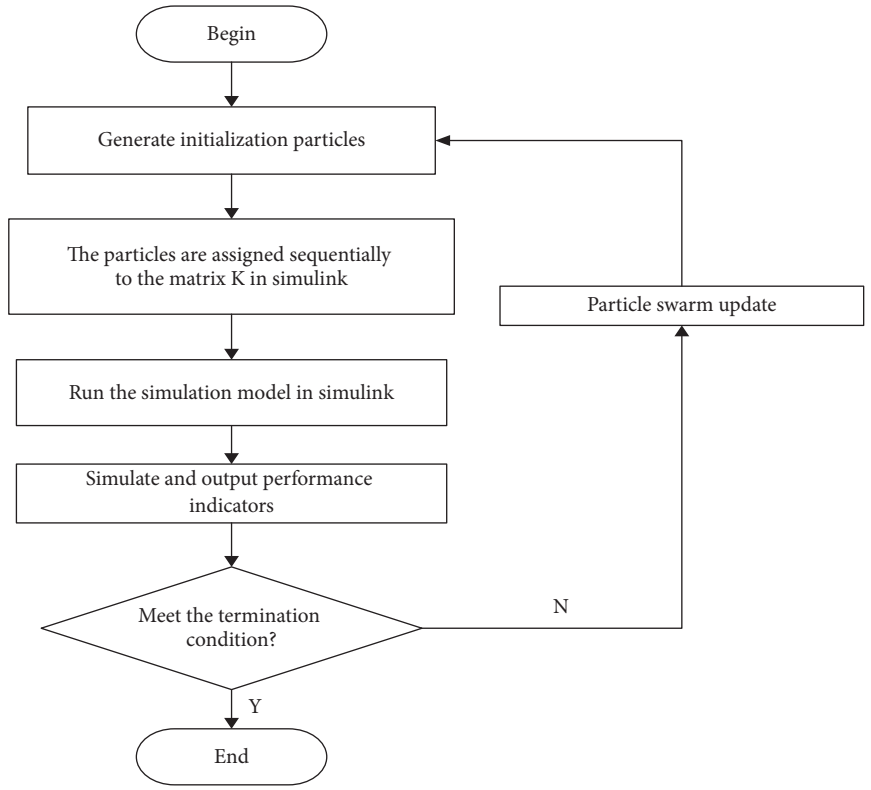

Figure 2: Algorithm flowchart.

This performance index is represented as

$$J = \int_0^\infty q_{11}\left(x_1 - x_d\right)^2 + q_{22}{x_2}^2 + q_{33}{x_3}^2 + q_{44}{x_4}^2 + ru^2\Big)\,dt \tag{50}$$

where q_{11}, q_{22}, q_{33}, and q_{44} are the weights of trolley position, trolley speed, swing angle position, and swing angle velocity, respectively. The weight matrices of LQR are usually obtained according to experience, which makes parameter selection more subjective, and the optimal response result cannot be achieved. Especially when there are more parameters, it is difficult to find better control parameters. Hence, in order to address the problem of LQR weight selection, PSO optimization algorithm is introduced.

PSO is an intelligent algorithm for simulating bird swarm's predator behavior. It has been widely used in many fields because of its simple concept, easy implementation, and fast convergence. Reference [38] uses a linear decreasing particle swarm algorithm to optimize the fuzzy controller for diabetes delayed model. PSO with random inertia weight is used to optimize fuzzy sliding mode for a class of nonlinear systems with structured and unstructured uncertainties in [39].

Suppose the number of particles of a population be m, and the search space is four- dimensional. The velocity and position of the ith particle are, respectively,

$$V = \left[v_{i1}, v_{i2}, v_{i3}, v_{i4}\right],$$
$$X = \left[x_{i1}, x_{i2}, x_{i3}, x_{i4}\right]; \tag{51}$$
$$i = 1, 2 \ldots m$$

The formula for updating the velocity and position of each particle is

$$V_i^{d+1} = \omega V_i^d + c_1 r_1\left(P_{bi}{}^d - X_i\right) + c_2 r_2\left(G_{bi}{}^d - X_i\right) \tag{52}$$

and

$$X_i^{d+1} = X_i^d + V_i^d \tag{53}$$

where V_i^d and X_i^d are the position vector and velocity vector of the ith particle in d generation, respectively,. ω is inertia weight, c_1 and c_2 are learning factors, r_1 and r_2 are random numbers between 0 and 1, and P_b^i and G_b^i are the position of the individual extreme point and the position of the global extreme point of the whole group after the d th iteration.

The flowchart for optimizing the LQR weight matrix Q with PSO is shown as Figure 2.

4. The Simulation Research

In this section, numerical simulation researches are carried out in the environment of Matlab/Simulink to test the performance of the proposed method. In the following simulations,

the parameter values for the crane system are selected as follows:

$$\begin{aligned} M &= 10kg, \\ m &= 5kg, \\ l &= 1m, \\ g &= 9.8m/s^2, \\ \mu &= 0.2 \end{aligned} \tag{54}$$

The desired position of the trolley is set to $x_d = 0.6m$. The initial value of the state variable is $\mathbf{x}_0 = [0 \ 0 \ 0.002 \ 0]$. The constraints $|\theta(t)| \le \theta_p = (\pi/12)(rad)$ and $|\dot{\theta}(t)| \le \theta_v = (\pi/4)(rad/s)$ are given by [36].

The particle swarm size used in the optimization is m=50, the maximum number of iterations is d=20, the inertia factor is $\omega = 0.6$, and the weight factor is $c_1 = c_2 = 2$. When R is selected as 1, the optimized matrix Q is

$$Q = [150, 19.1583, 11.7468, 1073.04] \tag{55}$$

The feedback gains of robust LQR controller based on two kinds of T-S models are calculated by LMIs. The feedback gains of the first method are

$$\begin{aligned} K_{11} &= 1.0e+03 \\ &\quad * [0.0548 \ \ 0.1657 \ \ -1.5930 \ \ -0.0259]; \\ K_{12} &= 1.0e+03 \\ &\quad * [0.0549 \ \ 0.1659 \ \ -1.5940 \ \ -0.0259]; \\ K_{13} &= 1.0e+03 \\ &\quad * [0.0593 \ \ 0.1772 \ \ -1.6380 \ \ -0.0147]; \\ K_{14} &= 1.0e+03 \\ &\quad * [0.0694 \ \ 0.2069 \ \ -1.9027 \ \ -0.0151]; \\ K_{15} &= 1.0e+03 \\ &\quad * [0.0527 \ \ 0.1593 \ \ -1.5310 \ \ -0.0247]; \\ K_{16} &= 1.0e+03 \\ &\quad * [0.0528 \ \ 0.1595 \ \ -1.5320 \ \ -0.0248]; \\ K_{17} &= 1.0e+03 \\ &\quad * [0.0572 \ \ 0.1708 \ \ -1.5786 \ \ -0.0141]; \\ K_{18} &= 1.0e+03 \\ &\quad * [0.0572 \ \ 0.1708 \ \ -1.5794 \ \ -0.0141]. \end{aligned} \tag{56}$$

The feedback gains of the second method are

$$\begin{aligned} K_{21} &= 1.0e+03 \\ &\quad * [0.0900 \ \ 0.2675 \ \ -2.4276 \ \ -0.13667]; \\ K_{22} &= 1.0e+03 \\ &\quad * [0.0902 \ \ 0.2678 \ \ -2.4301 \ \ -0.1368]; \\ K_{23} &= 1.0e+03 \\ &\quad * [0.0910 \ \ 0.2697 \ \ -2.4318 \ \ -0.1335]; \\ K_{24} &= 1.0e+03 \\ &\quad * [0.1066 \ \ 0.3153 \ \ -2.8349 \ \ -0.1521]; \\ K_{25} &= 1.0e+03 \\ &\quad * [0.0860 \ \ 0.2555 \ \ -2.3187 \ \ -0.1301]; \\ K_{26} &= 1.0e+03 \\ &\quad * [0.0862 \ \ 0.2561 \ \ -2.3233 \ \ -0.1305]; \\ K_{27} &= 1.0e+03 \\ &\quad * [0.0870 \ \ 0.2577 \ \ -2.3233 \ \ -0.1273]; \\ K_{28} &= 1.0e+03 \\ &\quad * [0.0870 \ \ 0.2577 \ \ -2.3233 \ \ -0.1274]. \end{aligned} \tag{57}$$

In order to evaluate the feasibility and validity of the proposed method, the simulations are given in three cases.

Case 1 (comparison study). In order to prove effectiveness of the controllers on the basis of the two kinds of T-S fuzzy model in this paper, control methods in [34, 37] are used to the overhead crane to make comparisons. The LQR method mentioned in [37] is designed based on linear models. In [34], the design of robust LQR controller is on the base of local approximate models. The feedback gain matrices obtained above are applied to the control systems, respectively. The target location is set to 0.6m. In order to study the rejected disturbance performance of the proposed control method, a pulse disturbance with an amplitude of 1.5 N is injected to the control input of the system between 15s and 15.3s. The simulation results are illustrated in Figure 3. In order to better evaluate and compare these methods, the important characteristics of each method are gathered in Table 1.

It is seen from Figure 3 that none of these four methods has any remaining swings in the target position. According to Table 1, using the proposed methods in this paper, the trolley can reach the target position in 9.2s and 9.3s, and the maximum swing angle is 0.95° and 1.005°, respectively. The trolley transportation time in [34, 37] is 10s and 11.7s, and the maximum swing angle is 1.275° and 2.498°. For the impulse disturbance, the maximum variation of load swing angle is 0.025° and 0.044° when the proposed methods are adopted, and the maximum variation of load swing angle is 0.135° and 0.272° when the literature method is used. The results show the proposed control methods can make the system have better rapidity, anti-swing, and rejected disturbance performance.

Case 2 (different transport distance). In order to verify the control performance of the proposed control method under

Table 1: Detailed quantified results of four methods.

Method	Transient process under given action				Transient process under pulse disturbance		
	Transportation time (s)	Maximum load swing angle (°)	Overshoot (%)	Trolley maximum speed (m/s)	Displacement change (m)	Transition time (s)	Maximum load swing angle (°)
The first method	9.2	0.95	0	0.136	0.005	5	0.025
The second method	9.3	1.005	0	0.142	0.002	5.1	0.044
Reference [34]	10	1.275	0	0.191	0.009	5.5	0.135
Reference [37]	11.7	2.498	0.27	0.225	0.0128	6.1	0.272

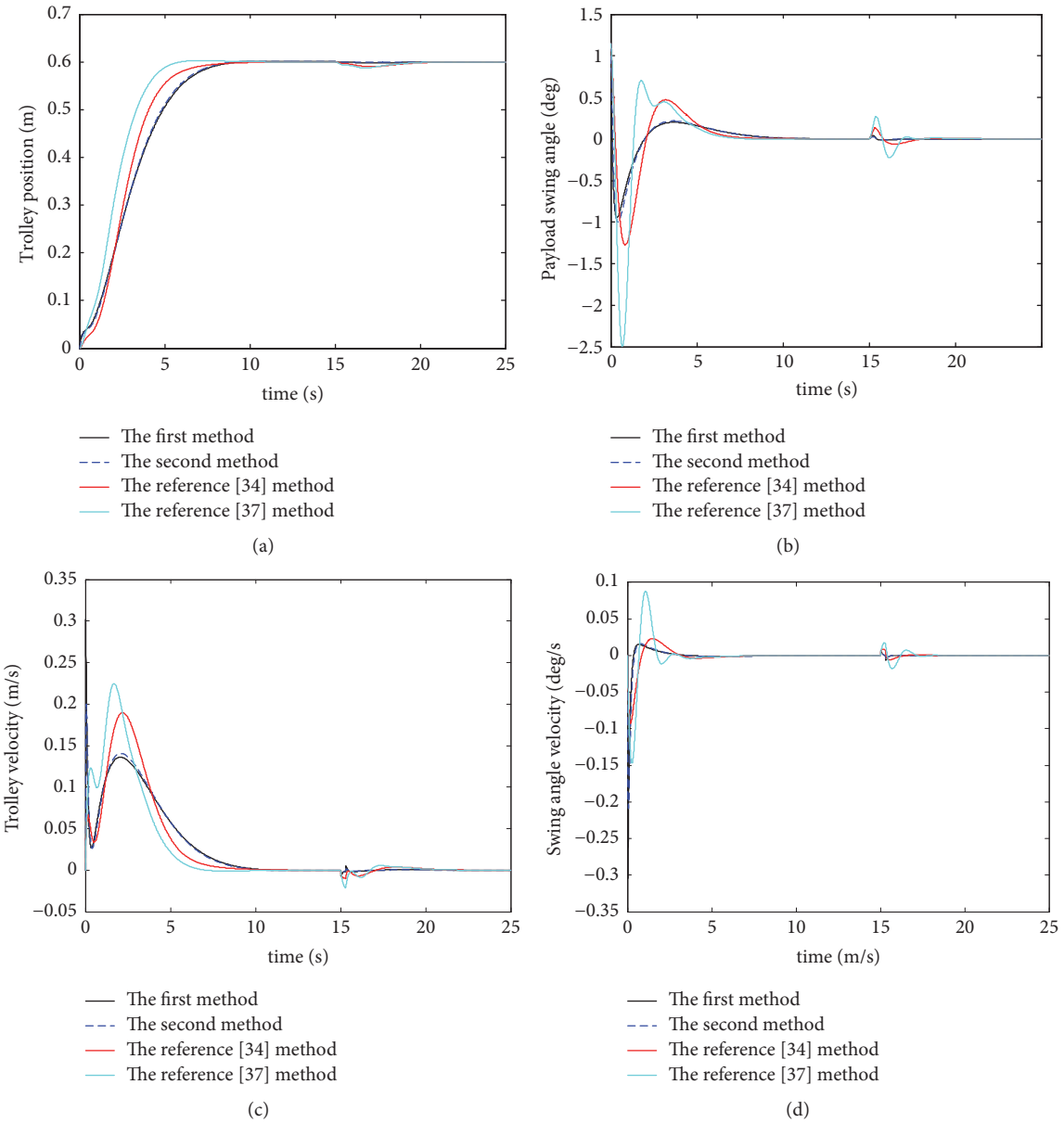

Figure 3: Comparison of different control methods.

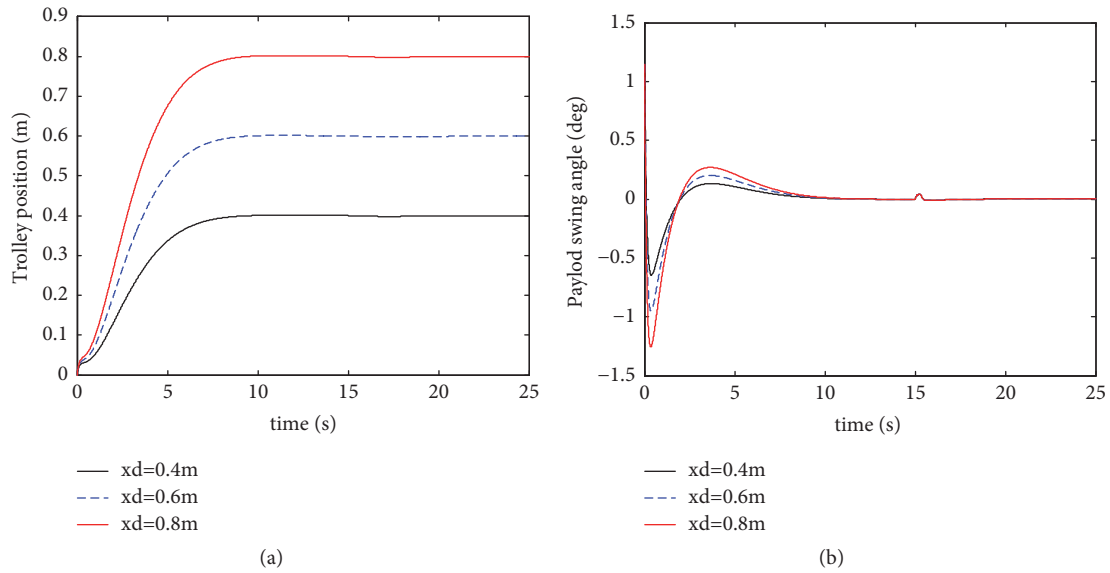

Figure 4: Response curve of different transformation distance x_d for the first method.

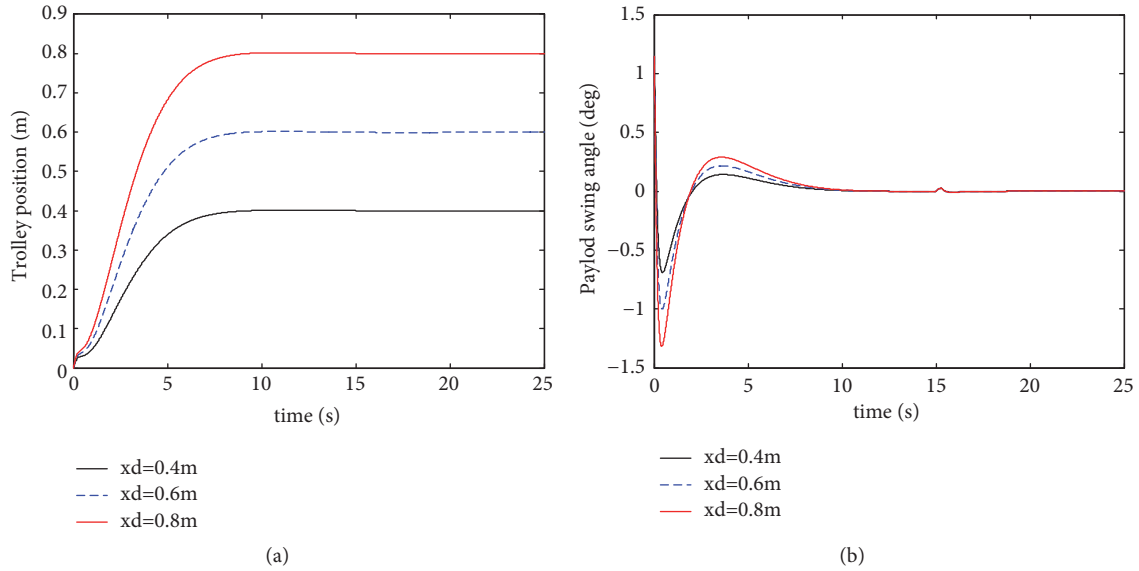

Figure 5: Response curve of different transformation distance x_d for the second method.

different transferring distances, the distances are selected to be $x_d = 0.4m, x_d = 0.6m$, and $x_d = 0.8m$, respectively. The simulation results for two control methods are given in Figures 4 and 5. From the simulation results, we can see that the trolley can reach the desired position accurately and the payload swing is suppressed well during the transportation process. The swing angle is between $[-1.5^\circ, 1.5^\circ]$ and it disappeared quickly after the trolley arrives at the target position. The rejected disturbance performance does not change with the change of desired position.

Figure 6 shows a more complex case that is close to practical case, the trolley moves 0.4m from the initial position, then moves 1.5m, and finally comes back to 1.1m.

As can be seen from Figure 6, the two control methods have good control performance.

Case 3 (robustness study). The payload mass and rope length are two important parameters that affect the system performance. In practical industrial applications, payload mass or rope length need be changed according to different transportation tasks. To examine the robustness of the system, various payloads and rope lengths are taken into account. In this text, the simulation results of the change of payload mass from 3 kg to 7 kg and the variation of rope length from 0.8m to 1.2m are given in Figures 7 and 8, respectively.

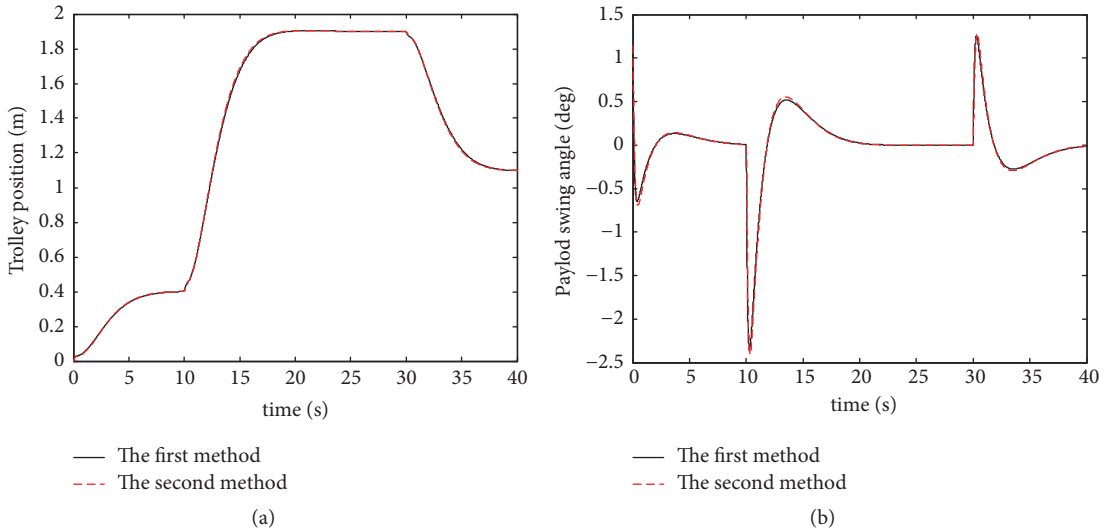

Figure 6: Trolley motion in different cases.

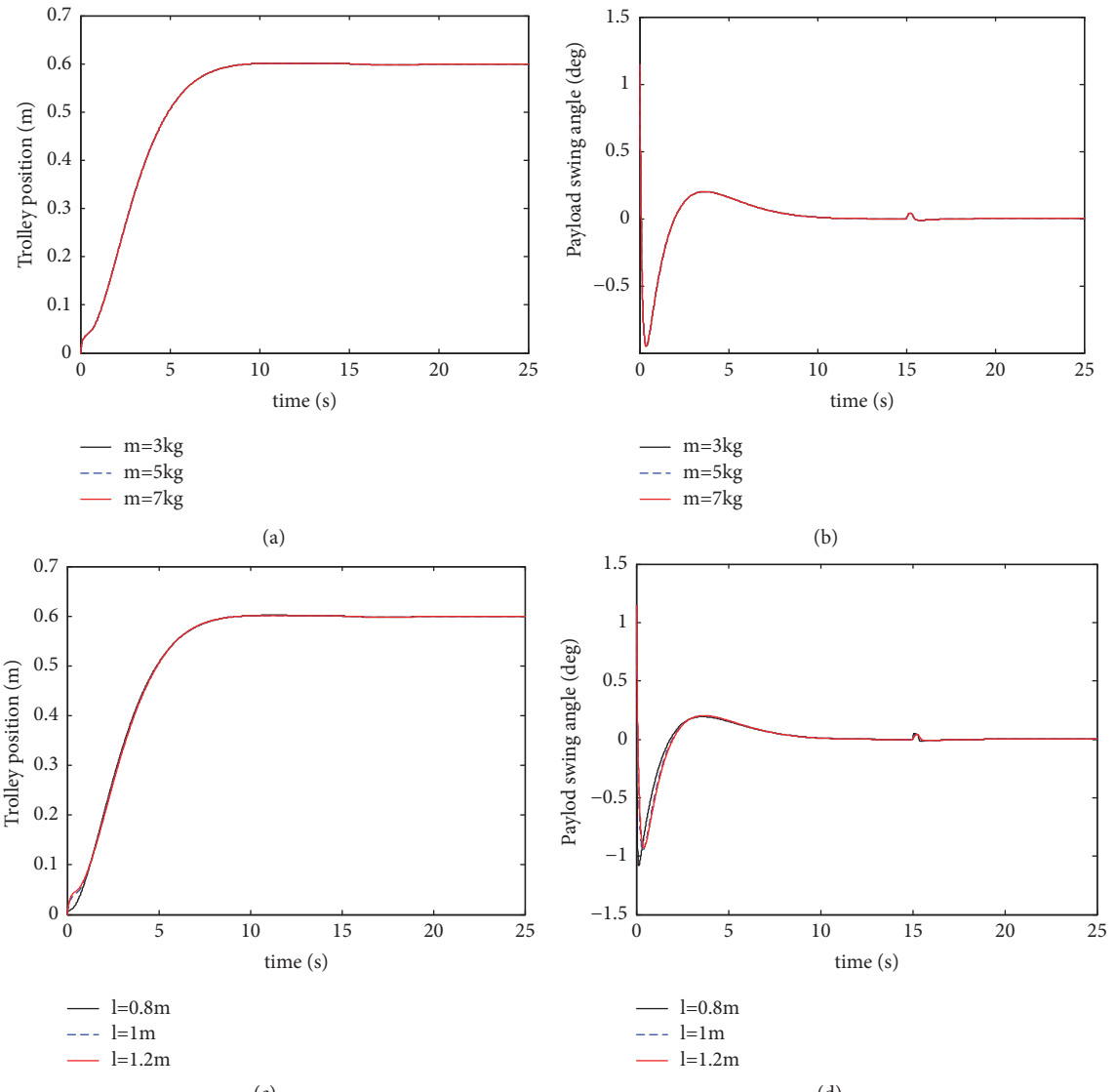

Figure 7: Response curves of different m and l for the first method.

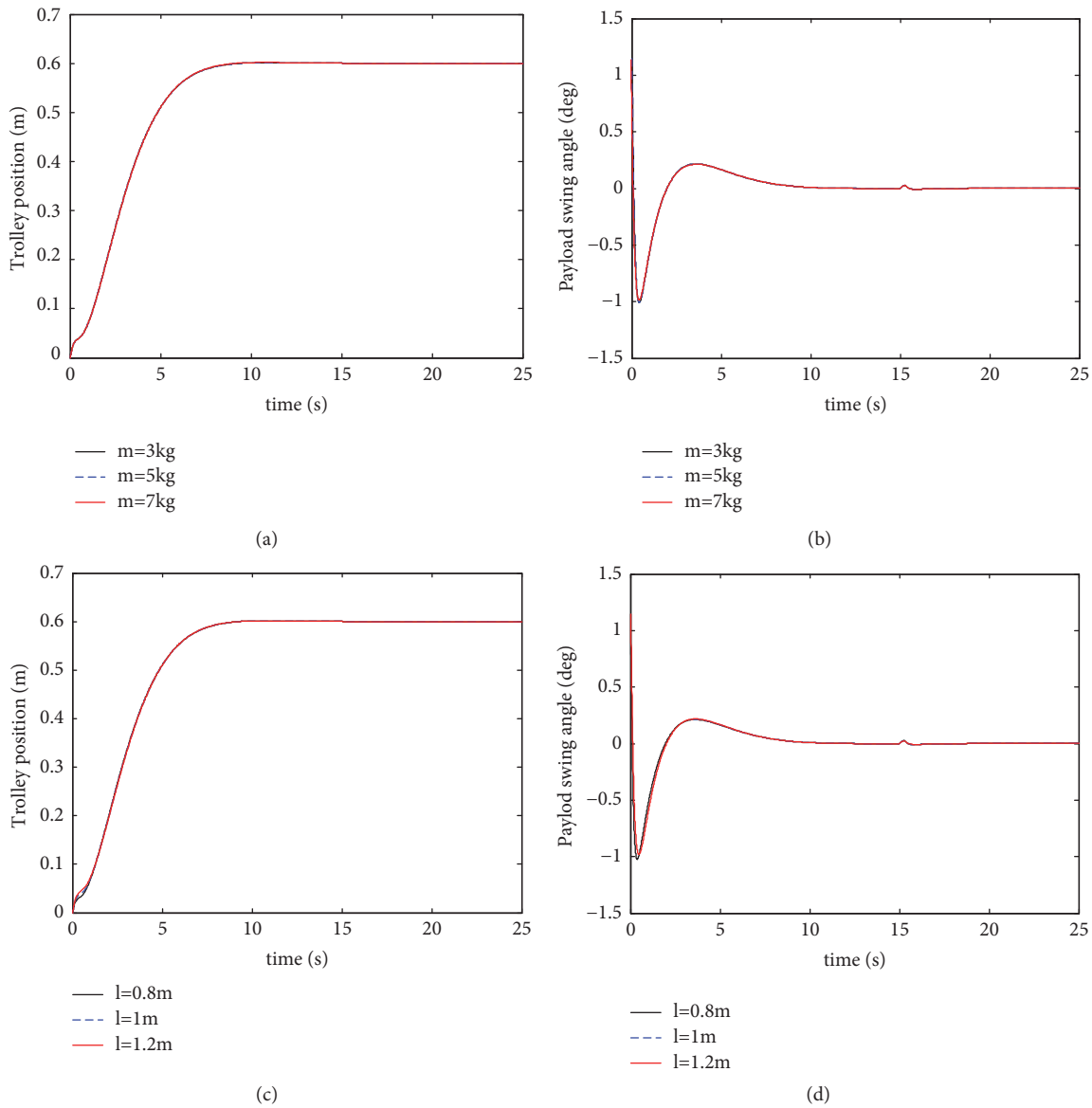

FIGURE 8: Response curves of different m and l for the second method.

According to Figures 7 and 8, it can be seen that fast performance of the trolley and payload swing angle are almost unchanged when load mass m changes. We can also know that the rapidity of the trolley changes little and the payload swing angle increases when the rope length l reduces, but the swing angle is within the allowable range. The interference suppression performance does not vary when the two parameters change. These results show that the proposed methods have strong robustness to the changes of the payload mass and rope length, which is very important in practice.

5. Conclusion

In this paper, the two T-S fuzzy models are established by using the virtual control variables and approximate method, and the nonlinear mathematical model of crane is replaced by T-S fuzzy model. In order to control the anti-swing and positioning of overhead crane, the robust LQR controller is designed on the basis of considering uncertain T-S model. The weights Q and R of LQR affect the feedback gain matrices, so PSO algorithm is proposed to optimize the weight Q. The simulation results of different control methods are compared, and the robustness to the variation of trolley mass, rope length, and external disturbance and rejected disturbance performance of the control system are discussed, respectively. The results showed that the proposed control methods had better control effect.

Nomenclature

T-S: Takagi-Sugeno
LQR: Linear quadratic regulator
PSO: Particle swarm optimization

LMI:	Linear matrix inequality
A_{li}, B_{li}, C_{li}:	Local T-S fuzzy matrices
M_{lk}, N_{lj}, C_{ln}:	Fuzzy membership functions associated with premise variables
z_{l1}, z_{l2}, z_{l3}:	Premise variables
$\mathbf{x}$:	State vector of the system
x_d:	Desired position of the trolley
μ:	Friction coefficient
ω_{li}:	Weight of ith rule
h_{li}:	Normalized weight of ith rule.

Data Availability

The data used to support the findings of this study are included in the Supplementary Materials (available here).

Conflicts of Interest

The authors declare that they have no conflicts of interest.

Acknowledgments

This work was supported in part by Youth Science and Technology Research Foundation of Shanxi Province under Grant 201701D221108 and in part by Shanxi Key Laboratory of Advanced of Advanced Control and Intelligent Information System 201805D111001.

Supplementary Materials

In this paper, two T-S fuzzy modeling methods based on sector nonlinear technique are proposed. Each fuzzy T-S model is composed of 8 linear models with certain weights such as (27) in the paper. The matrices Ai and Bi of these models are needed when writing programs to calculate the feedback gain matrices of robust LQR controller. So the exact values of these matrices are given in the additional file. *(Supplementary Materials)*

References

[1] L. Ramli, Z. Mohamed, and H. Jaafar, "A neural network-based input shaping for swing suppression of an overhead crane under payload hoisting and mass variations," *Mechanical Systems and Signal Processing*, vol. 107, pp. 484–501, 2018.

[2] M. J. Maghsoudi, Z. Mohamed, S. Sudin, S. Buyamin, H. Jaafar, and S. Ahmad, "An improved input shaping design for an efficient sway control of a nonlinear 3D overhead crane with friction," *Mechanical Systems and Signal Processing*, vol. 92, pp. 364–378, 2017.

[3] M. H. I. Ishak, Z. Mohamed, and R. Mamat, "Anti-sway control schemes of a boom crane using command shaping techniques," *Jurnal Teknologi (Sciences & Engineering)*, vol. 67, no. 5, pp. 49–58, 2014.

[4] N. Sun, Y. C. Fang, and H. Chen, "A new antiswing control method for underactuated cranes with unmodeled uncertainties: theoretical design and hardware experiments," *IEEE Transactions on Industrial Electronics*, vol. 62, no. 1, pp. 453–465, 2015.

[5] P. Wang, Y. Fang, and Z. Jiang, "A direct swing constraint-based trajectory planning method for underactuated overhead cranes," *Acta Automatica Sinica*, vol. 40, no. 11, pp. 2415–2419, 2014.

[6] N. Q. Hoang, S.-G. Lee, H. Kim, and S.-C. Moon, "Trajectory planning for overhead crane by trolley acceleration shaping," *Journal of Mechanical Science and Technology*, vol. 28, no. 7, pp. 2879–2888, 2014.

[7] H. I. Jaafar, S. Y. S. Hussien, R. Ghazali, and Z. Mohamed, "Optimal tuning of PID+PD controller by PFS for Gantry Crane System," in *Proceedings of the 10th Asian Control Conference, ASCC 2015*, pp. 1–6, Malaysia, June 2015.

[8] S. Y. S. Hussien, H. I. Jaafar, R. Ghazali, and N. R. A. Razif, "The effects of auto-tuned method in pid and pd control scheme for gantry crane system," *International Journal of Soft Computing and Engineering*, vol. 64, no. 6, pp. 121–125, 2015.

[9] M. Hamid, M. Jamil, S. O. Gilani et al., "Jib system control of industrial robotic three degree of freedom crane using a hybrid controller," *Indian Journal of Science and Technology*, vol. 9, no. 21, pp. 1–9, 2016.

[10] X. Wang, Z. Chen, and X. Shao, "Research on two degree of freedom internal model anti-swing control of bridge crane," *Journal of Taiyuan University of Science and Technology*, vol. 37, no. 5, pp. 337–341, 2016.

[11] N. Sun, Y. Fang, and X. Wu, "An enhanced coupling nonlinear control method for bridge cranes," *IET Control Theory Appl*, vol. 8, no. 13, pp. 1215–1223, 2014.

[12] L. A. Tuan, J. Kim, S. Lee, T. Lim, and L. C. Nho, "Second-order sliding mode control of a 3D overhead crane with uncertain system parameters," *International Journal of Precision Engineering and Manufacturing*, vol. 15, no. 5, pp. 811–819, 2014.

[13] L. A. Tuan, S. G. Lee, L. C. Nho, and H. M. Cuong, "Robust controls for ship-mounted container cranes with viscoelastic foundation and flexible hoisting cable," *Journal of Systems and Control Engineering*, vol. 229, no. 7, pp. 662–674, 2015.

[14] A. T. Le and S. Lee, "3D cooperative control of tower cranes using robust adaptive techniques," *Journal of The Franklin Institute*, vol. 354, no. 18, pp. 8333–8357, 2017.

[15] Z. Wu, X. Xia, and B. Zhu, "Model predictive control for improving operational efficiency of overhead cranes," *Nonlinear Dynamics*, vol. 79, no. 4, pp. 2639–2657, 2015.

[16] D. Jolevski and O. Bego, "Model predictive control gantry/bridge crane with anti-sway algorithm," *Journal of Mechanical Science and Technology*, vol. 29, no. 2, pp. 827–834, 2015.

[17] J. Kalmari, J. Backman, and A. Visala, "Nonlinear model predictive control of hydraulic forestry crane with automatic sway damping," *Computers and Electronics in Agriculture*, vol. 109, pp. 36–45, 2014.

[18] L. A. Tuan, H. M. Cuong, S. Lee, L. C. Nho, and K. Moon, "Nonlinear feedback control of container crane mounted on elastic foundation with the flexibility of suspended cable," *Journal of Vibration and Control*, vol. 22, no. 13, pp. 3067–3078, 2014.

[19] Q. Ngo and K. Hong, "Adaptive sliding mode control of container cranes," *IET Control Theory & Applications*, vol. 6, no. 5, pp. 662–668, 2012.

[20] L. A. Tuan, S. Lee, L. C. Nho, and D. H. Kim, "Model reference adaptive sliding mode control for three dimensional overhead cranes," *International Journal of Precision Engineering and Manufacturing*, vol. 14, no. 8, pp. 1329–1338, 2013.

[21] I. R. Ahmad, Y. Samer, and A. R. Hussain, "Fuzzy-logic control of an inverted pendulum on a cart," *Computers and Electrical Engineering*, vol. 61, pp. 31–47, 2017.

[22] B. Seyfi, B. Rahmani, A. H. D. Markazi, and V. S. Nasrabad, "Feedback linearrized-based and approximated parallel distributed compensation approach: theory and experimental implementation," *Majlesi Journal of Mechatronic Systems*, vol. 4, no. 4, pp. 7–16, 2015.

[23] M. S. Sadeghi and N. Vafamand, "More relaxed stability conditions for fuzzy TS control systems by optimal determination of membership function information," *Control Engineering and Applied Informatics*, vol. 16, no. 2, pp. 67–77, 2014.

[24] E. Mattar and H. Al-Junaid, "LMI LYapunov Based TS Fuzzy Modeling and Controller Synthesis for a Nonlinear and Beam System," in *Proceedings of ISER 4th International Conference*, pp. 77–82, 2015.

[25] M. U. Asad, J. Zafar, A. Hunif, U. Farooq, and J. Gu, "Fuzzy LMI Servo Controller for Uncertain Ball and Beam System," in *Proceedings of the 17th IEEE Internaional Multi Topic Conference*, pp. 360–365, 2014.

[26] N. Vafamand and M. Rakhshan, "Dynamic model-based fuzzy controller for maximum power point tracking of photovoltaic systems: A linear matrix inequality approach," *Journal of Dynamic Systems, Measurement, and Control*, vol. 139, no. 5, Article ID 051010-051010-6, 2017.

[27] P. Hušek and K. Narenathreyas, "Aircraft longitudinal motion control based on Takagi–Sugeno fuzzy model," *Applied Soft Computing*, vol. 49, pp. 269–278, 2016.

[28] N. Vafamand and M. Shasadeghi, "More relaxed non-quadratic stabilization conditions using TS open loop system and control law properties," *Asian Journal of Control*, vol. 19, no. 2, pp. 467–481, 2017.

[29] G. He, J. Li, P. Cui, and Y. Li, "T-S fuzzy model based control strategy for the networked suspention control system of maglev train," *Mathematical Problems in Engineering*, vol. 2015, Article ID 291702, 11 pages, 2015.

[30] M. H. Khooban, N. Vafamand, and T. Niknam, "T–S fuzzy model predictive speed control of electrical vehicles," *ISA Transactions*, vol. 64, pp. 231–240, 2016.

[31] M. H. Khooban, N. Vafamand, T. Niknam, T. Dragicevic, and F. Blaabjerg, "Model-predictive control based on Takagi-Sugeno fuzzy model for electrical vehicles delayed model," *IET Electric Power Applications*, vol. 11, no. 5, pp. 918–934, 2017.

[32] A. Elhamdaouy, I. Salhi, A. Belattar, and S. Doubabi, "Takagie Sugeno fuzzy modeling for three-phase micro hydropower plant prototype," *International Journal of Hydrogen Energy*, vol. 42, pp. 17782–17792, 2017.

[33] N. Vafamand, M. H. Asemani, and A. Khayatian, "TS fuzzy robust L 1 control for nonlinear systems with persistent bounded disturbances," *Journal of The Franklin Institute*, vol. 354, no. 14, pp. 5854–5876, 2017.

[34] G. Z. Zhou, M. Luo, and J. J. Li, "Anti-rocking and guaranteed performance control of container loading and unloading bridge based on T-S model," *Lifting the Transport Machinery*, pp. 34–37, 2007.

[35] G.-Z. Zhou and M. Luo, "Takagi-Sugeno model-based H-infinity anti-swing control for container crane," *Kongzhi Lilun Yu Yingyong/Control Theory and Applications*, vol. 25, no. 2, pp. 268–272, 2008.

[36] Y.-J. Chen, W.-J. Wang, and C.-L. Chang, "Guaranteed cost control for an overhead crane with practical constraints: fuzzy descriptor system approach," *Engineering Applications of Artificial Intelligence*, vol. 22, no. 4-5, pp. 639–645, 2009.

[37] N. Sun, Y.-C. Fang, and H. Chen, "Antiswing tracking control for underactuated bridge cranes," *Kongzhi Lilun Yu Yingyong/Control Theory and Applications*, vol. 32, no. 3, pp. 326–333, 2015.

[38] M. H. Khooban, D. N. M. Abadi, A. Alfi, and M. Siahi, "Swarm optimization tuned mamdani fuzzy controller for diabetes delayed model," *Turkish Journal of Electrical Engineering & Computer Sciences*, vol. 21, no. 1, pp. 2110–2126, 2013.

[39] M. H. Khooban and M. R. Soltanpour, "Swarm optimization tuned fuzzy sliding mode control design for a class of nonlinear systems in presence of uncertainties," *Journal of Intelligent & Fuzzy Systems: Applications in Engineering and Technology*, vol. 24, no. 2, pp. 383–394, 2013.